



Study of ph effect on AZ31 magnesium alloy corrosion for using in temporary implants

CAJ. da Silva¹; LNM. Braguin¹; LO. Berbel¹; BVG. de Viveiros¹; JL. Rossi¹; M. Saiki¹; I. Costa¹

*Corresponding author: E-mail address: caio.silva@ipen.br

Abstract: Currently, magnesium alloys are gaining great interest for medical applications due to their degrading properties in the human body ensuring a great biocompatibility. These alloys also provide profitable mechanical properties due similarities with human bone. However, a difficulty in applying these materials in the biomaterials industries is the corrosion prior to cell healing. The effect of the chemical composition of Mg alloys on their corrosion behavior is well known. In this study, samples of AZ31 magnesium alloy were cut into chips for elemental chemical analysis by neutron activation analysis (NAA). Concentrations of the elements As, La, Mg, Mn, Na, Sb and Zn were determined in the AZ31 alloy. Visualization tests of agar corrosion development in various media, of 0.90% sodium chloride solution (mass), phosphate buffer saline (PBS) and simulated body fluid (SBF) were performed. Visualizations of the effect of agar gel corrosion revealed pH variation during the corrosion process due to the released into the cathode. The highest released of hydroxyl ions occurred in NaCl solution compared to PBS and SBF solutions indicating that NaCl solution was much more aggressive to the alloy compared to the others.

Keywords: Biomaterials. Magnesium alloy. Neutron activation analysis. Corrosion.

Introduction

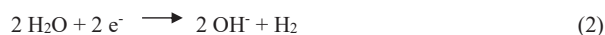
Considering the increase of biomaterials industry, the scientific community has searched about development of new types of these materials for biomedical applications, as well as for the improvement of the existing ones. Among these biomaterials, magnesium alloys have been proposed in this scenario as biodegradable metals for temporary implants, which avoids a new surgery for their removal¹, in the applications as cardiovascular stents and orthopedic prostheses.

This applicability is mainly due its intrinsic biocompatibility in the physiological environment since the major element (Mg) is a cofactor of more than 300 enzymatic reactions in the body, such as DNA, RNA and protein synthesis². Several studies have also reported additional benefits of magnesium such as antibacterial, osteoconductor and osteoinductor effect³.

Moreover, these alloys provide mechanical properties similar to the human bone which also avoids stress shielding phenomena⁴. However, magnesium alloys can quickly dissolve and corrode in aqueous solutions; especially those containing chloride ions⁵.

Rapid degradation rates in physiological medias are the main limitation for the use of these magnesium alloys, essentially in cases of degradation before cell healing⁶⁻⁸. Concerning to alloy elements and its impurities, it is known that they can form secondary particles, which may be nobler than the matrix, facilitating or inhibiting the degradation rate⁹.

The main chemical reactions that occur by Mg in contact with physiological media in the body are anodic reaction of Mg oxidation (1) and cathodic reaction of water reduction (2)²:



According to the reaction (2), Mg corrosion causes variation of the pH on the medium. Corrosion monitoring by means of pH measurements has been widely used in the study of magnesium degradation, although this kind of analysis usually brings only qualitative results. This is the cathodic reaction (Eq. 2) that can be used as an estimate to predict the overall corrosion rate based on the measurement of pH increase⁹.

Neutron Activation Analysis (NAA) was the analytical technique used to determine elements in this study to analyze Mg alloy composition, due to its advantages in the analysis of this type of materials such as high sensitivity, multi-element determination and the analyses of a great variety of matrices¹⁰.

The objective of this research was to determine the elemental composition of the AZ31 magnesium alloy by the NAA technique as well as to evaluate the variation of pH during the corrosion of this alloy in different simulated body solutions.

MATERIALS AND METHODS

Materials

The AZ31 magnesium alloy studied was imported to Alfa Aesar from Massachusetts, United States. This alloy was acquired in foil form with dimensions 30 cm x 30 cm and 1 mm thickness.

The preparation of the alloy for element determination

¹Instituto de Pesquisas Energéticas e Nucleares (IPEN – CNEN/SP)

was firstly to transform it in the form of chips with the aid of steel pliers. The cleaning of the chips to eliminate possible contaminants from the steel pliers was performed using acetone PA in beaker containing the chips and under agitation with a glass stick. The chips were separated from acetone. Then the purified water was added to the beaker, where alloy chips remained immersed for about two hours. The separation of the chips of the solution was carried out by filtration with filter paper. The filter paper containing the chips was put in a Petri dish, which was placed inside the laminar flow cabin for drying at room temperature.

Figure 1 shows the photograph of AZ31 alloy chips of dimensions of 0.2 to 1.0 cm used in the analysis.

The alloy sample for corrosion immersion tests was obtained by cutting the alloy with dimensions of 15 mm x 15 mm using a mechanical guillotine. Then the samples were submitted to cleaning using successively ethyl alcohol, acetone and purified water under agitation for about 15 minutes, in each of the reagents. To obtain smooth and uniform surfaces, the alloys were grinded using silicon carbide paper of #500, #800, #1200, #2000 and #4000 granulometry successively. Ethyl alcohol was used to clean the alloy surface between the steps of the grinding and, in the final steps, with distilled water followed by drying with hot air jet.



Figure 1. Photograph of the chips obtained from AZ31 alloy.

Source: CAJ, Silva.

Simulated body solutions were used in *in vitro* tests of the electrochemical reactions with the AZ31 magnesium alloy. The solutions of 0.90% sodium chloride (mass), phosphate buffered saline (PBS) and simulated body fluid (SBF) are those commonly used in this corrosion studies of biomaterials¹¹⁻¹³ and were adopted in this work. The reagents used in the preparation of these solutions are presented in Table 1.

The PBS solution was prepared using 9.0 g of sodium chloride, 1.42 g of dibasic sodium phosphate and 2.72 g of monobasic potassium phosphate dissolved and diluted to 1000 mL of purified water. Regarding to SBF solution, its preparation was carried out according to Kokubo e Takadama¹⁴ with the exception of the water used, the purified water in the Millipore purification system was used instead of distilled water.

Methods

Procedure of neutron activation analysis (NAA)

For NAA, 50 mg of alloy chips were weighed in polyethylene envelopes and irradiated in the IEA-R1 reactor along with synthetic element standards. These standards were prepared pipetting single or multielemental standard solutions in sheets of filter paper.

Details about experimental procedure used for NAA as well as about analytical quality control of the results are presented in a previous work¹⁵.

The concentrations of the elements were calculated by the comparative method¹⁶ using the following equations.

$$C_a = \frac{m_p \cdot A_a \cdot e^{0,693(ta-tp)t_{1/2}}}{M_a \cdot A_p} \quad (3)$$

where C_s is the element concentration in the sample; m_{st} is the mass of the element in the standard; A_s and A_{st} are counting rates of the radioisotopes in the sample and in the standard, respectively; t_s and t_{st} are decay times for the sample and standard, respectively; M_s is the total mass of the sample and $t_{1/2}$ is the half-life of the radionuclide.

Table 1. Reagents used in the preparation of the simulated body solutions of 0.90% in mass of NaCl, phosphate buffered saline (PBS) and simulated body fluid (SBF).

Solution	Reagents	Molecular formula	Purity (%)
NaCl/ PBS/ SBF	Sodium chloride	NaCl	≥99.0
SBF	Potassium chloride	KCl	≥99.0
PBS	Bibasic sodium phosphate	Na ₂ HPO ₄	≥99.0
PBS	Monobasic sodium phosphate	KH ₂ PO ₄	≥99.0
SBF	Sodium hydrogen carbonate	NaHCO ₃	≥99.7
SBF	Tri-hydrated potassium phosphate	K ₃ PO ₄ · 3 H ₂ O	≥99.0
SBF	Hexahydrate magnesium chloride	MgCl · 6 H ₂ O	≥99.0
SBF	Hydrochloric acid	HCl	36.5 – 38
SBF	Calcium chloride	CaCl ₂	≥96.0
SBF	Sodium sulfate	Na ₂ SO ₄	≥99.0
SBF	Tris-hydroxymethyl aminomethane (Tris)	C ₄ H ₁₁ NO ₃	≥99.0

Procedure used for corrosion visualization test in agar-agar gel

Firstly, the areas of the alloy samples to be exposed to corrosion were delimited to 1 cm² using biological wax to avoid preferential corrosion at the edges (crevice). The agar-agar used was the bacteriological type of Kasvi K25-1800 and for its preparation 1.5 grams of agar-agar was used for 50 mL solution¹⁷.

For this preparation, each one of the solutions (0.90% in mass of NaCl, PBS and SBF) was heated to boiling temperature (100 ± 2) °C in a beaker of 50 mL. In this heated solution, 1.5 g of agar-agar and 5 mL of phenolphthalein indicator were added and with the aid of a glass stick, the solutions were homogenized and transferred into a Petri dish containing an alloy sample.

Procedure for corrosion monitoring by global pH measurement

The pH variation of the solution in contact with magnesium alloy sample was performed for different times at room temperature. For this, alloy samples with an area of 2.2 cm² were immersed in each one of the solutions NaCl, PBS and SBF. The test was performed in plastic Falcom tube with the capacity of 15 mL and the volume of each solution was of 11 mL. The ratio between solution volume and exposed alloy area was 5 mL/cm².

The pH measurements were performed using KASVI K39-2014B bench-type pHmeter and this test was performed in duplicate, and the mean value of pH measurements was used in the evaluation.

RESULTS AND DISCUSSION**Element determination in the AZ31 magnesium alloy**

Table 2 shows the results of determinations in the AZ31 magnesium alloy sample by NAA, as well as the results of detection limit of Cu, Fe and Ni elements, not detected in the analysis. The detection limits of these three elements were evaluated since they are commonly present in metal alloys and, in addition the alloy specification sheet shows only their maximum values.

Table 2. Concentrations of elements obtained in the AZ31 magnesium alloy by NAA.

Element	M \pm SD ^a	RSD ^b , %	Reference ¹⁸
Al, %	3.06 \pm 0.19	6.1	2.5 – 3.5
As, $\mu\text{g g}^{-1}$	2.30 \pm 0.34	14.8	–
Cu, %	< 0.012	–	<0.05
Fe, %	< 0.095	–	<0.005
Mg, %	96.5 \pm 4.2	4.4	Remainder
Mn, %	0.325 \pm 0.013	3.9	0.2 – 1.0
Ni, %	< 0.037	–	<0.005
Na, $\mu\text{g g}^{-1}$	397 \pm 32	8.1	–
Sb, ng g^{-1}	275 \pm 56	20.4	–
La, ng g^{-1}	316 \pm 16	5.2	–
Zn, %	1.009 \pm 0.045	4.5	0.6 – 1.3

a. arithmetic mean and standard deviation from 2 to 4 determinations; b. relative standard deviation.

Table 2 shows that the concentrations of elements Al, Mn and Zn are within the ranges of specification/reference values and, in addition, four other elements were detected and quantified: As, Na, Sb and La. The relative standard deviations of the determinations were less than 15.0 %, with the exception of Sb, that presented RSD of 20.4 % due to its low concentration in the alloy.

Results of the corrosion visualization tests in agar-agar gel

In Figures from 2 to 4, the images of corrosion visualization in agar-agar before and after exposure are presented with the test solutions containing phenolphthalein as the acid-base indicator.

For the test in sodium chloride solution, (Fig.2) the alloy is shown (a) prior to exposure to the test solution and, (b) after immersion. The pink coloration is due to the formation of hydroxyl ions (OH⁻) resulting from the cathodic reaction. The pink color is instantly evidenced in a large surface area, as well as the formation of H₂ bubbles. It can be seen that the pink coloration intensifies (after one hour) (c) and coloration propagates throughout the surface area (after two hours), (d).

In the PBS medium (Fig.3), in (a) the AZ31 alloy sample prior to immersion is shown, and large formation of H₂ bubbles is observed over much of the sample in (b), evidencing a high reactivity of the alloy in this medium. After five hours of test the H₂ bubbles remained(c). However, only after 24 hours of assay (d) a slight pink coloration was indicated due to low rates of cathodic oxygen reduction reaction.

As in previous cases, in the SBF medium (Fig.4) there is an instantaneous formation of H₂ bubbles on the surface and also the presence of pink staining regions in (b). The intensification of OH⁻ formation gradually increased after one hour (c) and five hours of test (d), where the staining remained during 24-hour monitoring.

This visualization test allowed identifying the preferred cathodic regions in the early stages of corrosion from the main water reduction reaction (Eq. 2). It is noted in Fig 2 that in sodium chloride solution, after two hours of immersion, the identification and differentiation of the anodic and cathodic regions are hard to be identified due to intense corrosion attack and large release of hydroxyl ions.

Results of corrosion monitoring by global pH measurements

The results of pH measurements in sodium chloride solution, PBS and SBF during 5 days of test in duplicate are shown in Figure 5. It is observed that the pH of the medium varies faster and more intensely in the case of the NaCl medium, showing that it corresponds to the most aggressive medium among the tested.

The curves of pH variation with exposure time in PBS and SBF solutions showed similar behavior for these solutions, i.e., continuous pH increase from the beginning to the end of test, generally in the order of 2 units. In the sodium chloride solution, the pH increase was about six pH units (from 4.43 to 10.79). Additionally, between 1 and 3 hours of test there was an abrupt and significant increase in pH. It should be noted that in SBF, the pH reached values close to those observed in the sodium chloride solution at the end of the test, after 5 days.

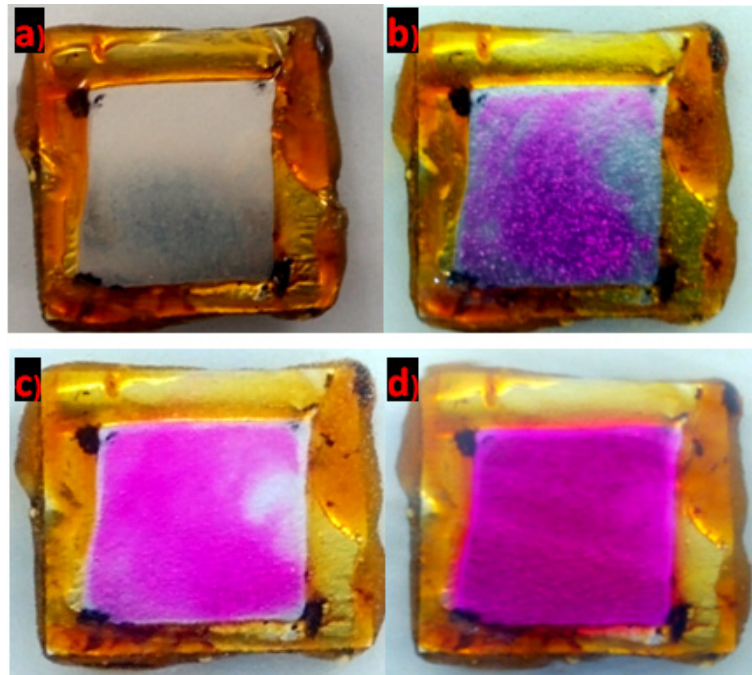


Figure 2. Photographs of the AZ31 alloy in 0.90 wt. % sodium chloride agar–agarcontaining phenolphthalein for different immersion periods; photos of sample (a) prior to immersion, (b) just after immersion, (c) after an hour of immersion and (d) after two hours of immersion.

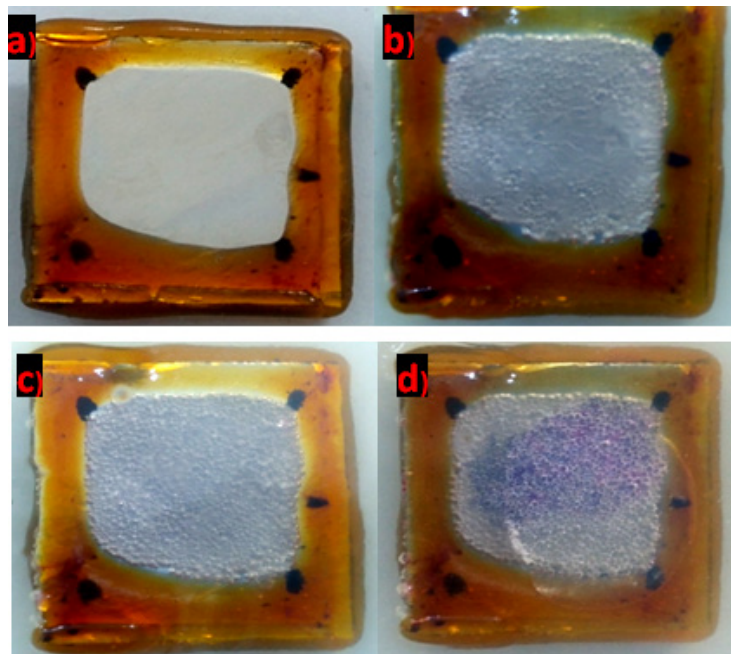


Figure 3. Photographs of the AZ31 alloy in PBS agar–agar containing phenolphthalein for different immersion periods; photos of sample (a) prior to immersion, (b) just after immersion, (c) after an hour of immersion and (d) after one day of immersion.

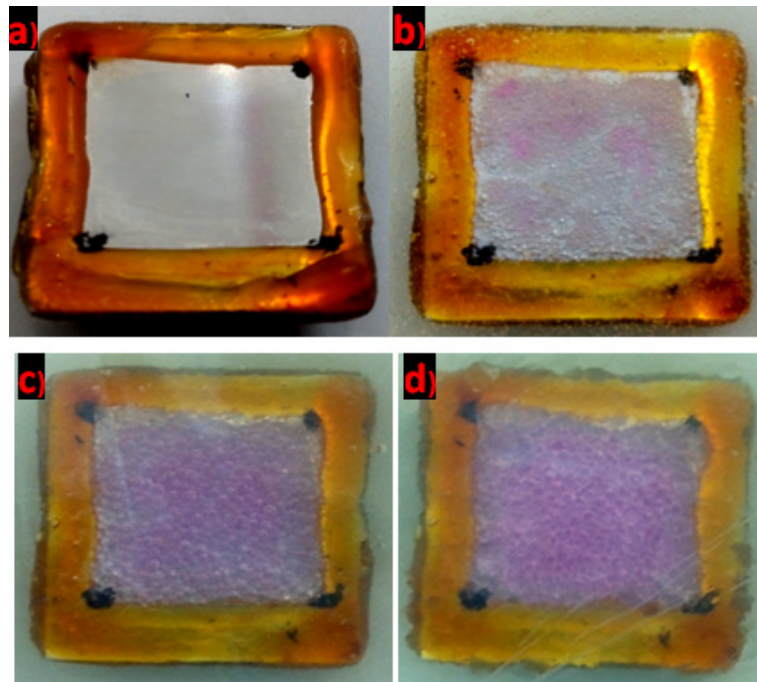


Figure 4. Photographs of the AZ31 alloy in SBF agar–agar containing phenolphthalein for different immersion times; photos of sample (a) prior to immersion, (b) just after immersion, (c) after an hour of immersion and (d) after five hours of immersion.

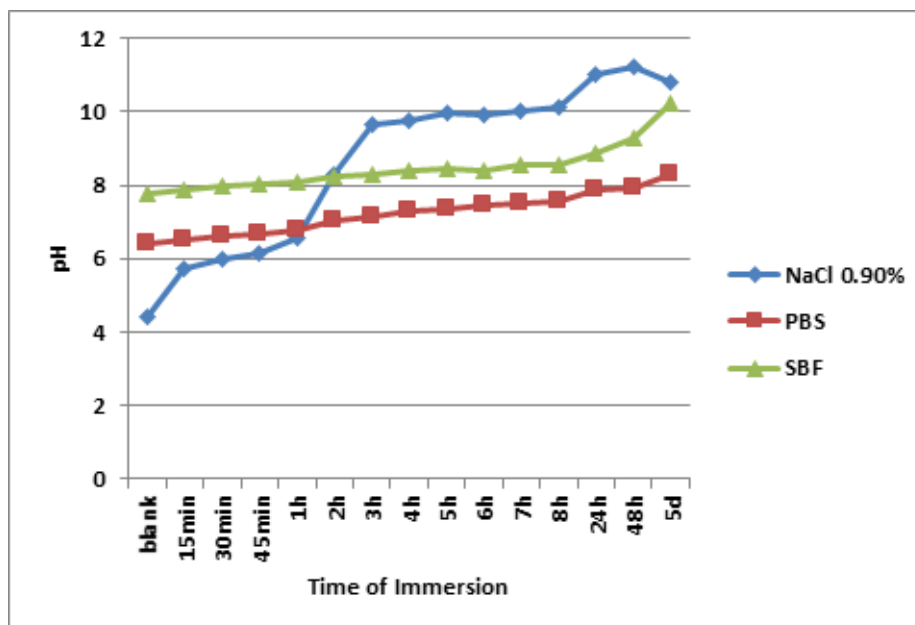


Figure 5. Curves of pH variation with time of exposure of AZ31 samples to simulated body solutions.

Conclusions

Neutron activation analysis of AZ31 magnesium alloy showed that concentrations of Al, Mn and Zn are within the ranges stipulated by the supplier specification. Four elements (As, La, Sb and Na) not presented in this specification were determined by the NAA technique.

Visualization of color change in the agar–agar and the pH variation with time of test revealed high susceptibility of the tested alloy to corrosion since the first times of exposure and demonstrated a difference in intensity depending on the type of simulated body solution used. Sodium chloride solution was the medium with the highest activity resulting in the largest production of hydroxyl ions (OH⁻) among those produced in PBS and SBF solutions. On the other hand, the PBS solution was the least aggressive among the solutions tested.

Acknowledgments

The authors are grateful to São Paulo Research Foundation (FAPESP–BRAZIL) and National Council for Scientific and Technological Development (CNPq–BRAZIL) for the financial support and the author C.A.J. Silva are also grateful to Co-ordination for the Improvement of Higher Education Personnel (CAPES–BRAZIL) for his grant.

References

- [1]. Sezer N, Evis Z, Kayhan SMA, Koc Tahmasebifar M. Review of magnesium–based biomaterials and their applications. *J Magnes Alloy* 6: 23–43 (2018).
- [2]. Gu XN, Lo SS, Li XM., Fan YB. Magnesium based degradable biomaterials: a review. *Front Mater Sci* 8: 200–218 (2014).
- [3]. Jung O, Smeets R, Porchetta D, Kopp A, Ptock C, Müller U, Heiland M, Schwade M, Behr B, Kroeger N, Kluwe L, Hanken H, Hartjen P. Optimized in vitro procedure for assessing the cytocompatibility of magnesium–based biomaterials. *Acta Biomater* 23: 354–363 (2015).
- [4]. Shaw BA. Corrosion resistance of magnesium alloy in *ASM Handbook 13A – Corrosion: fundamentals, testing and protection*, ed by SD Cramer and BS Covino. ASM International, United States, p. 692 (2003).
- [5]. Ding W. Opportunities and challenges for the biodegradable magnesium alloys as next generation biomaterials. *Regen. Biomater*, 3: 79–86 (2016).
- [6]. Li X, Liu X, Wu S, Yeung KWK, Zheng Y, Chu PK. Design of magnesium alloys with controllable degradation for biomedical implants: from bulk to surface. *Acta Biomater* 45: 2–30 (2016).
- [7]. Tan L, Wang Q, Lin X, Wan P, Zhang G, Zhang Q, Yang K. Loss of mechanical properties in vivo and bone–implant interface strength of AZ31B magnesium alloy screws with Si–containing coating, *Acta Biomater* 10: 2333–2340 (2014).
- [8]. Pardo A, Merino MC, Coy AE, Arrabal R, Viejo F, Matykina E. Corrosion behavior of magnesium/aluminum alloys in 3.5% wt. NaCl. *Corros Sci* 50: 823–834 (2007).
- [9]. Kirkland N, Birbilis N, Staiger M. Assessing the corrosion of biodegradable magnesium implants: a critical review of current methodologies and their limitations. *Acta Biomater* 8: 925–936 (2012).
- [10]. Ehmman WD and Vance DE. *Radiochemistry and Nuclear Methods of Analysis*. 1st ed. John Wiley & Sons, Inc; New York, 1991. 560 p.
- [11]. Thirumalaikumarasamy D, Shanmugam K, Balasubramanian V. Comparison of the corrosion behaviour of AZ31B magnesium alloy under immersion test and potentiodynamic polarization test in NaCl solution, *J Magnes Alloy* 2: 36–49 (2014).
- [12]. Fue S, Gao H, Chen G, Gao L, Chen X. Deterioration of mechanical properties for pre–corroded AZ31 sheet in simulated physiological environment. *Mater Sci Eng*, 593: 153–162 (2014).
- [13]. Xue D, Yun Y, Tan Z, Dong, Z, Schulz MJ. In vivo and in vitro degradation behaviour of magnesium alloys as biomaterials, *J Mater Sci Technol* 28: 261–267 (2011).
- [14]. Kokubo T, Takadama H. How useful is SBF in predicting in vivo bone bioactivity? *Acta Biomater* 27: 2907–2915 (2006).
- [15]. Silva CAJ, Costa I, Rossi JL, Saiki M. Determination of chemical elements in magnesium–based materials by neutron activation analysis, *Proc. International Nuclear Atlantic Conference INAC 2019 Santos, Brazil* (2019).
- [16]. De Soete D, Gijbels R, Hoste J. *Neutron Activation Analysis*. Wiley–Interscience, London (1987).

- [17]. Bugarin AFS (2017). Study of corrosion resistance of 2024-T3 and 7475-T651 aluminium alloys by friction stir welding (FSW) [thesis]. São Paulo: Nuclear and Energy Research Institute; 2017.
- 18]. Alfa Aesar by Thermo Fisher Scientific. 44009 Magnesium Aluminum Zinc foil (2018), available at: <https://www.alfa.com/pt/catalog/044009/>> [accessed 5 July 2018].